Tamap Journal of Physical Science
http://www.tamap.org/

TJOPS-1812-07
Volume 2018, Article ID 4
Research Article

Thermodynamic Properties of Cavities in Hot X-ray Plasma: A2556

Muhammed Kıyami Erdim [1, 2 *] and Murat HÜDAVERDİ [2]

[1] *Graduate School of Natural and Applied Sciences, Yıldız Technical University, Istanbul 34220, Turkey*
[2] *Physics Department, Faculty of Science and Art, Yıldız Technical University, Istanbul, 34220, Turkey*

Received: 07.12.2018 • **Accepted**: 20.12.2018 • **Published Online:** 26.12.2018

Abstract: We present X-ray wavelength analysis results of A2556 galaxy cluster. The observation was made by *Chandra* observatory with 20 ksec exposure time. A2556 is located in the Aquarius super cluster region with a redshift value of z=0.0871. The previous studies report the existence of possible sub-structures. We detected X-ray cavities in the hot plasma around the center of the cluster. We calculated thermo−dynamical properties of cavities to see how they affect the intra-cluster medium. Our results show that the cavities have higher metal abundance and entropy than ambient medium, which indicates that the origin of the cavities might be AGN activity.

Keywords: High energy astrophysics: galaxies: active, X-rays: galaxies

1. INTRODUCTION

The clusters of galaxies are the most massive gravitationally bounded structures in the universe. It is widely accepted that the AGN activities plays a major role in the evolution process of these celestial objects. They contribute to the heating of the ICM by producing jets and hot bubbles. These AGN interactions can be observed as x-ray cavities and surface brightness discontinuities (Sonkamble et al. 2015; Nulsen et al. 2005). It is also discovered that the AGN outburst can affect the general properties of a cluster, not only central region (Gitti et al. 2007). Metal-rich gas can be injected through this process and contribute to the redistribution of elements (Tozzi et al. 2015; Mernier et al. 2015).

This active state of the AGNs is thought to be triggered by the binding energy of the accreting matter that fuels its supermassive black hole (SMBH). When the ICM cools down by radiation, accreting matter rate increases, which triggers the AGN activity. It releases its energy by creating jets and hot bubbles, which heats the ICM and drops the accretion rate. And the radiative cooling processes dominate again. Although this energy transfer process is not fully understood yet, this cycle covers the main steps (Patermo et al. 2014).

In this work we present the thermodynamical properties of X-ray plasma cavities detected around the central galaxy of A2556 galaxy cluster. The cluster hosts a weak shock created by non-merger mechanisms (Qin Z. et al. 2013). Position of the shock coincides with the cavity direction. In the following sections, we present the observation information and data reduction methods in Section 2, analysis steps in the subsections, with a brief conclusion in Section 3. Throughout the study, we adopt the cosmological parameters H_0=68.7, Ω_M=0.308, Ω_Λ=0.692, All quoted errors are derived at the 68 % confidence level, unless otherwise is stated.

2. DATA REDUCTION and ANALYSIS

A2556 was observed by Chandra Observatory with ~20ks exposure time on 2001/10/05 (Obs.ID. 2226) in VFAINT mode. The observation was made with ACIS-S detector and the object is centered on S3 chip. Therefore, we

* Correspondence: kiyami_erdim@hotmail.com

primarily focus on the S3 chip. The analysis software and the versions of CIAO v4.9 software, HEAsoft v6.22.1 and CALDB v4.7.7 are used during the research. We followed the standard data reduction routine and removed bad pixels, and columns. The raw data was reprocessed by *chandra-repro* to create level 2-event file. After cleaning procedure, the total filtered effective exposure time is 19.9 ksec. An exposure corrected, adaptively smoothed 0.5 − 7 keV image is shown in the left panel of Figure 1. Right panel shows Aquarius super cluster central crowded region with A2556 close neighbors of A2554 at northwest and A2550 at southwest by ASCA GIS X-ray data. The image is from the archival database (http://darts.jaxa.jp/astro/asca/data/index.html).

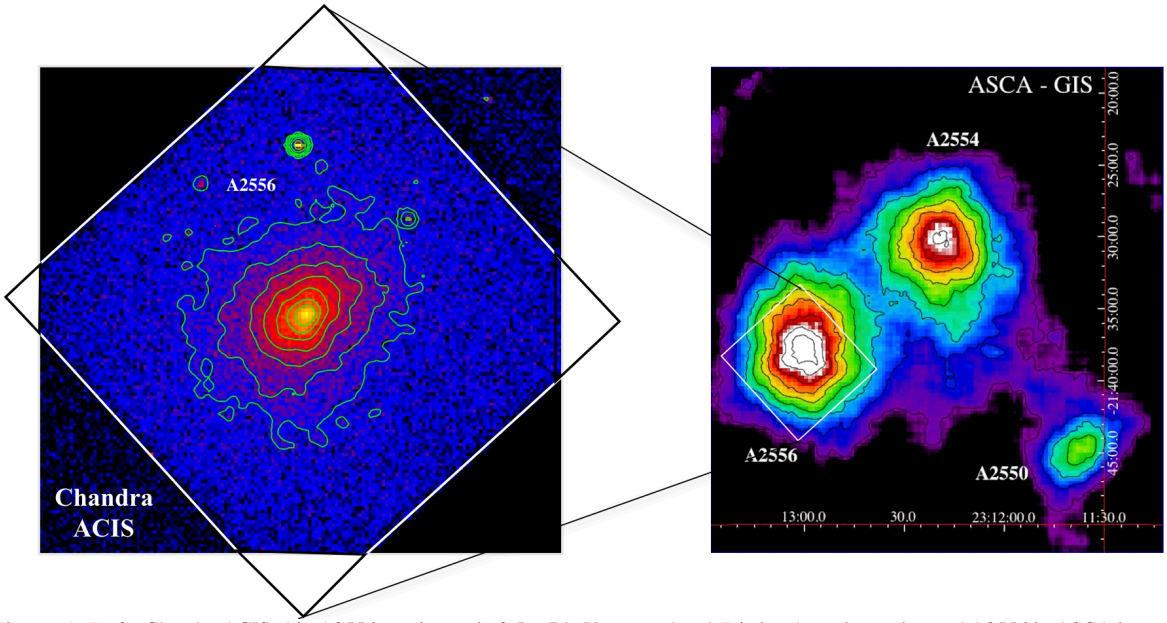

Figure 1: Left: Chandra ACIS chip A2556 raw image in 0.5 – 7 keV energy band. **Right**: Aquarius region and A2556 in ASCA image.

For spectral and further imaging analysis, we masked any X-ray point sources which is significant at 4 σ confidence level. Point source detection was performed by using the CIAO *wavdetect* tool in the 0.5−7 keV energy band. After masking procedure, the holes are filled with a locally estimated background from the vicinity of each point sources which is performed by using the CIAO tool *dmfilth*. The blank sky observation, which is a stack of observations of X-ray source free regions in the sky, is used as the background data. Quite often the blank sky spectrum must be normalized to the source spectrum in order to express appropriate background at the sky position. For this purpose we use the 10 − 12 keV energy internal in the outer part of the observation. Figure 2, shows A2556 temperature (red) and metal abundance (green) radial profile.

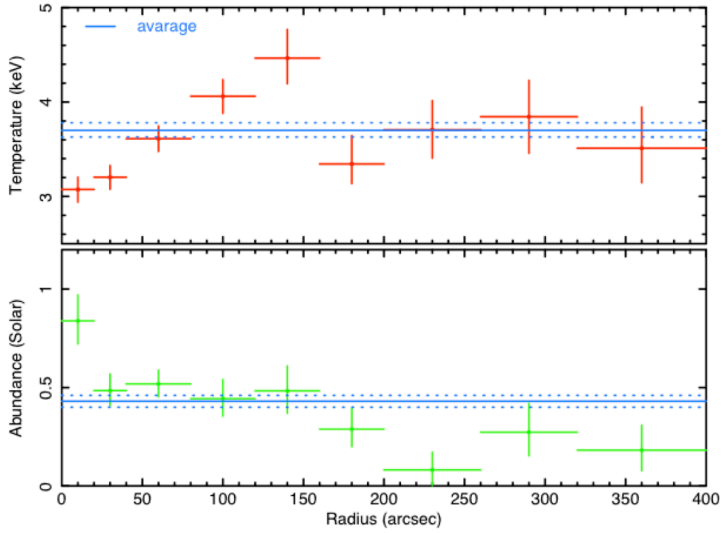

Figure 2: A2556 temperature (red) and metal abundance (green) radial profile. The blue solid and dotted lines represent the hot X-ray plasma average values are related error range.

2.1 Morphological Parameters

Dynamical disturbances like deviation from symmetry and/or the displacement of cluster core are reliable indicators for recent merger events. Therefore to classify the clusters morphology is very crucial and provides critical information. We used two methods to define A2556 morphology: the emission centroid shift (Mohr et al. 1993; O'hara et al. 2006; Poole et al. 2006; Maughan et al. 2008, 2012) and the brightness concentration parameter (Santos et al. 2008). The centroid shift, *w*, is defined by consecutive circles centered on the peak, and increased by 5% steps from R_{ap}, by following the formula;

$$w = \left[\frac{1}{N-1}\sum(\Delta_i - \langle\Delta\rangle)^2\right]^{1/2} \times \frac{1}{R_{ap}},$$

where Δ_i is the distance between the peak and the centroid of the i^{th} aperture. The surface brightness parameter, *c*, is defined as the ratio of the peak to the interested annular. We computed the centroid shift till the radius of 400 kpc;

$$c = \frac{SB(r < 40\ kpc)}{SB(r < 400\ kpc)}$$

By using the above equations, we calculated the centroid shift and concentration parameters. We used the definitions and methods described in (Haines et al. 2012; Koulouridis et al. 2014). Centroid shift parameter is an indicator of disturbance of a cluster. Disturbed clusters have high centroid shift value. Dynamical processes like mergers, in-falling sub-groups or ANG activities not only effect the symmetric distribution of gas and increase centroid shift value, they also disrupts the cooling flow and dissipates the cold plasma located around the core. Level of this dissipation can be measured by concentration parameter. The definition of concentration parameter is the surface brightness ratio of the central area over the ambient medium. Clusters with compact cool-cores have higher concentration parameters. By following the above-mentioned definitions, A2556 has a minor disturbance with w=0.014 ± 0.002 centroid-shift value and a compact core with c=0.236 ± 0.023 concentration parameter value.

2.2. Imaging Analysis

AGN activities in relaxed clusters can cause cavities by ejecting high-energy plasma with jets. When the plasma heats up to the higher energies, these regions can be seen as cavities in x-ray band (Sonkamble et al. 2015). In order to detect possible cavities, we created unsharp-masked image of the cluster with the method described in Sonkamble et al. (2015). Unsharp-masked image is obtained by subtracting two images of the cluster. First image is smoothed with a wide Gaussian kernel (4 σ) in order to reveal the large-scale features while erasing small-scale features. Second image is smoothed with a narrow Gaussian kernel (12 σ) to preserve small-scale features. By subtracting these two images, we are able to reveal the x-ray cavities in the ICM. Exposure corrected and background subtracted images of the cluster are used for this method, and smoothed with the *aconvolve* task of CIAO. Cavities are detected around the Brightest Central Galaxy (BCG) of the A2556. These cavities might be caused by AGN activity. The weak shock, which is detected in previous studies (Qin Z. et al. 2013) is in the direction of the cavities. High-energy jets can be the origin of weak shocks. The X-ray plasma cavities in A2556 are shown in Figure 3 by green regions.

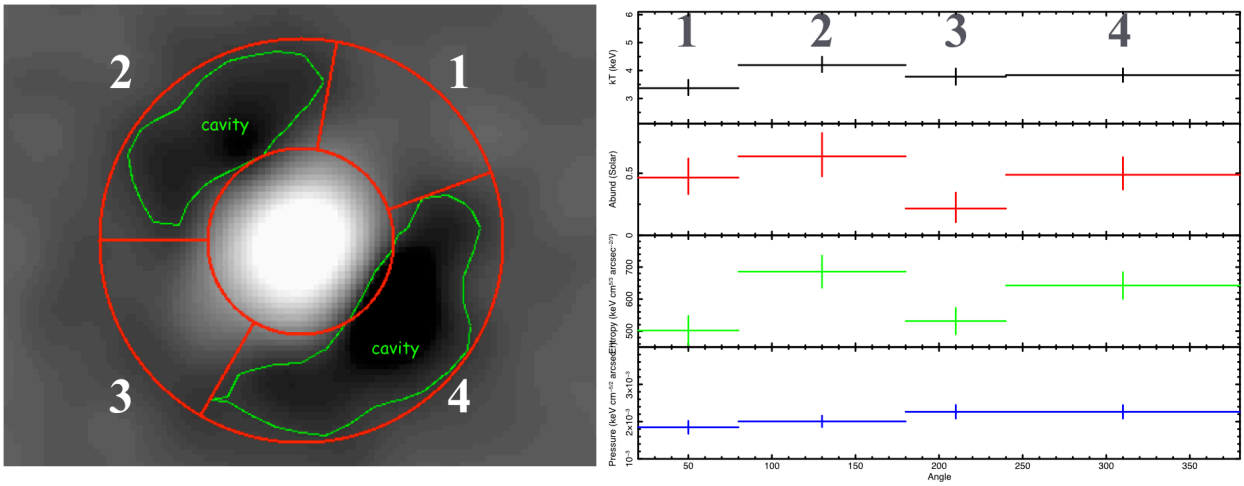

Figure 3: A2556 X-ray plasma cavities (left) and thermo−dynamical properties of four sectors (right).

2.3. Thermo−dynamical Calculations

We examined the thermo−dynamical properties of cavities. In order to do that, we selected annuli shaped area and divided it into four sectors. The selections were based upon approximate cavity shapes. Inner radius of the annuli is 30 arcsec and the outer radius is 65 arcsec. The regions are covering two cavities and two non-cavity control areas, for comparison. Figure 3 show the selection of four sectors and the X-ray plasma cavities. Right panel represents the thermo−dynamical values for each sector; temperature, abundance, pressure and entropy values of each sector.

Temperature and abundance values are derived from the spectral fitting. The pressure and entropy values are calculated with the method described in Botteon et al. (2018). We detected systematic increase in the abundance and entropy values of cavities compared to non-cavity regions. This increment can be explained by AGN bubble injection, which transfers the metals from rich-core to the outer regions of the cluster (Tozzi et al. 2015; Mernier et al. 2015). We couldn't find any significant correlation with temperature and pressure values among cavity / non-cavity areas. The cavity regions are labeled as 2 and 3 for the visual aid.

3. CONCLUSION

Strong AGN activities usually create radio lobes around the core (Cassano et al. 2010, Bottoen et al. 2018). Ogrean et al. (2015) showed that A2556 doesn't have radio lobes that can be related with an AGN injection. Since the lifetime of these kind of radio emissions are relatively short (Chenhao et al. 2016). And thus, the cavity properties of A2556 can be explained by a weak AGN activity or remnants of an older activity.

Acknowledgements: MKE would like to acknowledge financial support from the Scientific and Technological Research Council of Turkey (TÜBİTAK) project number 113F117.

REFERENCES

[1] Ashby M. L. N. et al., 2013, ApJS, 209, 22
[2] Almeida C., Pérez García A. M., Acosta-Pulido J. A. 2009, AJ, 137, 179
[3] Sonkamble, S.S., Vagshette, N.D., Pawar, P.K. et al. Astrophys Space Sci (2015) 359: 61.
[4] P. E. J. Nulsen, B. R. McNamara, M. W. Wise, and L. P. David, ApJ (2005) 628:629-636
[5] M. Gitti, B. R. McNamara, P. E. J. Nulsen, and M. W. Wise, ApJ (2007), 660:1118Y1136
[6] P. Tozzi, F. Gastaldello, S. Molendi, et al. A&A (2015) 580, A6
[7] Paterno-Mahler R., Randall S. W., Bulbul E. F. et. Al, 2014 ApJ 791 104
[8] Qin Z., Xu H., Wang J., Wang Y., Gu J., Wu X. 2013, ApJ, 762, 22
[9] F. Mernier, J. de Plaa, L. Lovisari, et. al A&A (2015) 575, A37
[10] J. S. Santos, P. Rosati, P. Tozzi, H. Böhringer, S. Ettori, A. Bignamini, A&A (2008) 483, 35-47
[11] R. Cassano, S. Ettori, S. Giacintucci, et. al , ApJL (2010), 721:L82–L85
[12] A. Botteon, F. Gastaldello, G. Brunetti, MNRAS(2018) 476, 5591-5620
[13] G. A. Ogrean, R. J. van Weeren, C. Jones, et. al , ApJ (2015), 812:153
[14] Chenhao Zhang, Haiguang Xu, Zhenghao Zhu, et. al , ApJ (2016), 823:116
[15] Liyi Gu, Haiguang Xu, Junhua Gu, et. al , Apj (2009), 700:1161–1172
[16] G. Brunetti, G. Setti, L. Feretti, G. Giovannini, MNRAS (2001), 320:365-378
[17] Mohr, J. J., Fabricant, D. G., & Geller, M. J. 1993, ApJ, 413, 492
[18] O'Hara T. B., Mohr J. J., Bialek J. J., Evrard A. E., 2006, ApJ, 639, 64
[19] Poole G. B., Fardal M. A., Babul A., et al. 2006, MNRAS, 373, 881
[20] Maughan B. J., Jones C., Forman W., Van Speybroeck L. 2008, ApJS, 174, 117
[21] Santos J. S., Rosati P., Tozzi P., Bo¨hringer H., Ettori S., Bignamini A. 2008, A&A, 483, 35